1.1. Overview and principles of powder diffraction

R. E. DINNEBIER AND S. J. L. BILLINGE

1.1.1. Information content of a powder pattern

The structures of real materials comprise not only the crystal structure – the time- and space-averaged periodic configuration of atoms on an idealized periodic lattice – but also the microstructure, which is caused by imperfections, dislocations and all kinds of disorder. The microstructure is often responsible for interesting properties of the material. A powder diffraction pattern contains a wealth of information about this microstructure in addition to the average crystal structure, as shown schematically in Fig. 1.1.1.

At each stage of a powder diffraction study, great effort and ingenuity are needed to find the optimal experimental conditions and to understand and analyse the resulting line shapes and signals. As experimental equipment, theoretical understanding and computational tools have improved, it has become possible to tap into the rich information content of the line peak shapes and diffuse background of a typical powder diffraction pattern, yielding unprecedented information about real materials for materials scientists, chemists, physicists, earth scientists and engineers. For example, in the modern practice of whole-pattern modelling, the line profile is calculated from first principles, taking into account all aspects of the state of the sample, such as particle-size distributions, inhomogeneous strains and texture, as well as the experimental setup and aberrations. There is a useful feedback effect in that better profile descriptions result in more accurate determinations of the intensities of the Bragg peaks, which is important to extract accurate structural information (Bragg peaks are introduced in detail in the next section). Similarly, great progress has been made in the extraction of information from the diffuse signal that used to be called the 'background'. Rather than fitting the background using arbitrary fitting parameters, as is done in a traditional Rietveld refinement, careful corrections can be made for experimental effects such as Compton scattering, fluorescence, multiple scattering and scattering from sample environments. The resulting 'background' beneath and between the Bragg peaks of the corrected data is information-rich diffuse scattering from the sample, which contains information about the local structure and how it deviates from the average crystal structure in the form of defects and correlated lattice dynamics (phonons). Total-scattering methods that include both the Bragg and diffuse scattering are only now being fully appreciated, with quantitative analyses being carried out in real space using the atomic pair distribution function (PDF) method, and in reciprocal space with Monte Carlo simulated-annealing-type modelling based on the Debye equation.

In this introductory chapter, the basic physics behind the observation of a powder diffraction pattern is described. In accordance with the scheme in Fig. 1.1.1, the information in a powder diffraction pattern can be described by the Bragg-peak positions, the peak profile, the Bragg-peak intensities and the non-Bragg-scattering contributions to the background. After describing the fundamentals of scattering by a crystalline powder, the chapter is organized such that each of the paths illustrated in Fig. 1.1.1 is followed and described in an introductory way. Detailed descriptions of the state of the art in the kinds of studies covered in Fig. 1.1.1 can be found in following chapters, but here we discuss each aspect of powder diffraction in turn, giving a high-level overview of what information is available from powder diffraction as well as explaining the fundamental origin of the features containing that information. We do not attempt to review applications of the different kinds of studies, leaving that to the following chapters.

In this chapter we have drawn heavily on information within three textbooks (Dinnebier & Billinge, 2008; Mittemeijer & Welzel, 2012; Egami & Billinge, 2013) and references therein.

Figure 1.1.1
Schematic picture of the information content of a powder pattern. [Reproduced from Dinnebier & Billinge (2008) with permission from the Royal Society of Chemistry.]

1.1.2. The peak position

1.1.2.1. *The Bragg equation derived*

The easiest way to understand the structural information contained in powder diffraction, and historically one of the first ways in which diffraction was described, is *via* the well known Bragg equation (Bragg, 1913), which describes the principle of X-ray diffraction in terms of the reflection of X-rays by sets of lattice planes.

To understand the concept of a lattice plane, first imagine a three-dimensional periodic lattice of points, for example the corners of an array of cubes stacked in three dimensions. We can imagine a particular plane through the lattice by placing each layer of the stack of cubes on a tray: the tray then defines a lattice plane. Now imagine making the tray thinner and thinner until it
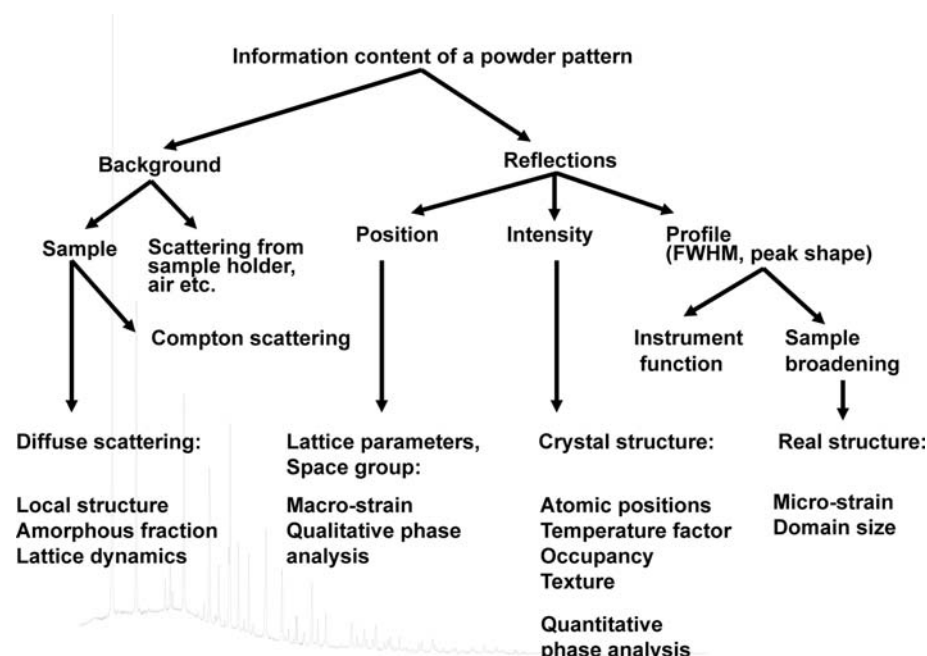
is infinitely thin, but still goes through the same set of points (the cube corners). What we see is that there is not just a single plane, but a series of equivalent planes: for example, between the top and second layers, the second and third layers, and so on. Each plane is parallel to the others and subsequent planes are separated by the same distance (the height of the cube). This is a set of lattice planes. We can also envisage inserting the trays in other ways. For example, we could place the trays vertically rather than horizontally and running from the left side to the right side of the stack of cubes, or alternatively running from the front of the stack to the back of the stack. Each of these is a different set of lattice planes (Fig. 1.1.2), although in this case they have the same layer spacing, or periodicity. If we were able to insert the tray at different angles to the cubes, for example at 45°, we could find other sets of parallel planes that, when we force them to go through some well defined subset of the points defining the lattice, will have well defined layer spacings or periodicities. Bragg's law showed that the diffraction pattern could be understood in terms of X-rays reflecting specularly off subsequent planes in each of these sets of planes and emerging in phase. (In reality, the actual effect is not specular reflection of light from an abstract plane, but a diffraction effect. However, the combination of diffraction and periodicity results in a selection rule that intense scattering only occurs when this particular specular-reflection condition holds.)

There are actually an infinite number of lattice planes in an infinite lattice, and it is important to have a way of labelling them, which is commonly done using the triplet of indices hkl, called Miller indices, where h, k and l are integers, and the separation of the planes is denoted by the distance d_{hkl}. When h, k and l have small values the planes are said to be 'low-order' planes. Low-order planes have the largest interplanar separations, and for a particular symmetry of the lattice there is a direct relationship between the Miller indices and d_{hkl}.

The Bragg equation gives the condition that must hold for specular reflection from subsequent planes in a set to be perfectly in phase, as illustrated in Fig. 1.1.3. It is evident in Fig. 1.1.3 that the wave reflecting off the lower plane travels a longer distance (by PN before and NQ after reflection occurs) than the wave reflecting off the upper plane. The two waves are in phase, resulting in constructive interference, only when $\Delta = |PN| + |NQ|$ is a multiple $n = 0, 1, 2, \ldots$ of the wavelength λ,

$$\Delta = n\lambda. \qquad (1.1.1)$$

In all other cases, destructive interference results, since it is always possible to find a deeper plane, p, for which the relation
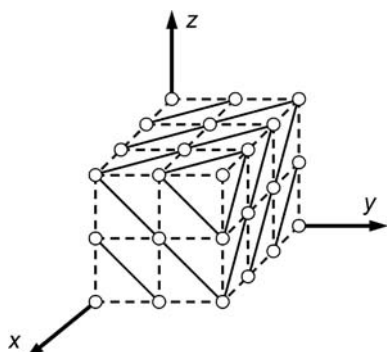

Figure 1.1.2
Schematic drawing of a set of parallel lattice planes (111) passing through all points of the cubic lattice.
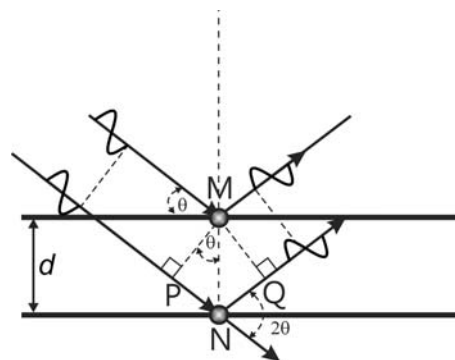

Figure 1.1.3
Illustration of the geometry used for the simplified derivation of Bragg's law. [Reproduced from Dinnebier & Billinge (2008) with permission from the Royal Society of Chemistry.]
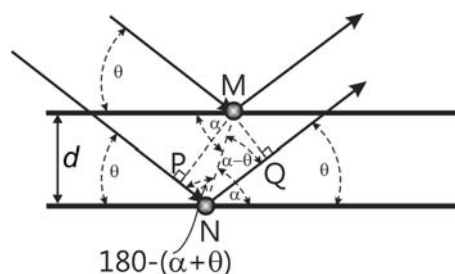

Figure 1.1.4
Illustration of the geometry in the general case where scattering takes place at the position of atoms in consecutive planes. [Reproduced from Dinnebier & Billinge (2008) with permission from the Royal Society of Chemistry.]

$p\Delta = n\lambda + 1/2$ exactly holds, giving rise to perfect destructive interference. Thus, when a narrow beam of X-rays impinges on a crystalline sample, sharp peaks in the intensity of the scattered X-rays are seen only at the angles for which equation (1.1.1) holds, with no intensity observed at other angles. As can easily be seen from Fig. 1.1.3, geometrically,

$$\Delta = 2d \sin \theta, \qquad (1.1.2)$$

where d is the interplanar spacing of the parallel lattice planes and 2θ is the diffraction (or 'scattering') angle, the angle between the incoming and outgoing X-ray beams. The angle $\theta = 2\theta/2$ is often called the Bragg angle. Combining equations (1.1.1) and (1.1.2) we get

$$n\lambda = 2d \sin \theta, \qquad (1.1.3)$$

which is the Bragg equation (Bragg, 1913).

This simplified derivation of the Bragg equation is often reproduced in textbooks. Although it leads to the correct solution, it has a serious drawback. In reality the X-rays are not reflected by planes, but are scattered by electrons bound to the atoms in the sample. The planes within a crystal are not like shiny optical mirrors, but contain discrete atoms separated by regions of much lower electron density and, in general, the atoms in one plane will not lie exactly above atoms in the plane below as implied by Fig. 1.1.3. How is it then that the simplified picture shown in Fig. 1.1.3 gives the correct result? A more general description shows that equation (1.1.3) is also valid if the atom in the lower lattice plane in Fig. 1.1.3 is shifted by an arbitrary amount within the plane (Fig. 1.1.4).

The phase shift can immediately be deduced from Fig. 1.1.4 as

$$n\lambda = \text{MN} \cos[180° - (\alpha + \theta)] + \text{MN} \cos(\alpha - \theta)$$
$$= \text{MN}[-\cos(\alpha + \theta) + \cos(\alpha - \theta)]. \qquad (1.1.4)$$

Using the standard trigonometric results

$$\cos(\alpha + \theta) = \cos\alpha\cos\theta - \sin\alpha\sin\theta,$$
$$\cos(\alpha - \theta) = \cos\alpha\cos\theta + \sin\alpha\sin\theta, \qquad (1.1.5)$$

equation (1.1.4) becomes

$$n\lambda = MN(2\sin\alpha\sin\theta) \qquad (1.1.6)$$

with

$$d = MN\sin\alpha, \qquad (1.1.7)$$

which may be substituted to yield the Bragg equation:

$$n\lambda = 2d\sin\theta. \qquad (1.1.8)$$

The Bragg equation holds for any radiation or particle that is used to probe the structure of the sample: X-rays, neutrons or electrons. Another equivalent, and highly useful, form of the Bragg equation for the particular case of X-rays is

$$Ed = \frac{6.199}{\sin\theta} \text{ with } \lambda = \frac{12.398}{E}, \qquad (1.1.9)$$

where the energy E of the X-rays is in keV and λ is in ångströms.

The Bragg law results in narrow beams of high intensity that emerge from the crystal in specific directions given by the Bragg equation, resulting in sharp spots on the detector, and there is a one-to-one correspondence between these Bragg spots (often referred to as Bragg reflections) and each set of crystallographic planes. Each Bragg spot is therefore labelled with the same set of Miller indices, hkl, as the set of planes that gave rise to it.

It is possible to construct a 'reciprocal space' where the axes of the space are in units of inverse length. The reference coordinate frame of the reciprocal space is defined by a set of basis vectors whose directions are perpendicular to the plane normals of the (100), (010) and (100) planes of the crystal. Thus, a *point* in this reciprocal space corresponds to a *direction* in direct space and every allowed reflection according to the Bragg law is represented by a point in reciprocal space. The set of points arising from the Bragg law forms a lattice in reciprocal space, which is called the 'reciprocal lattice', and each single crystal has its own reciprocal lattice. [See *International Tables for Crystallography* Volume B (Shmueli, 2008) for more details.]

To derive the Bragg equation, we used an assumption of specular reflection, which is borne out by experiment: for a crystalline material, destructive interference eliminates scattered intensity in all directions except where equation (1.1.3) holds. Strictly this holds only for crystals that are infinite in extent and which the incident X-ray beam can penetrate without loss of intensity. This does not sound like a particularly good approximation, but in practice it holds rather well. Even a fairly low energy X-ray beam that only penetrates, say, a micrometre into the material will still probe ~10 000 atomic layers. The condition is not strictly obeyed in the presence of defects and disorder in the material. In such materials the Bragg peaks are modified in their position, their width and their shape, and there is also an additional component of the diffracted intensity that may be observed in all directions, away from reciprocal-lattice points, known as diffuse scattering.

1.1.2.2. *The Bragg equation from the reciprocal lattice*

Here we develop in more detail the mathematics of the reciprocal lattice. The reciprocal lattice has been adopted by crystallographers as a simple and convenient representation of the physics of diffraction by a crystal. It is an extremely useful tool
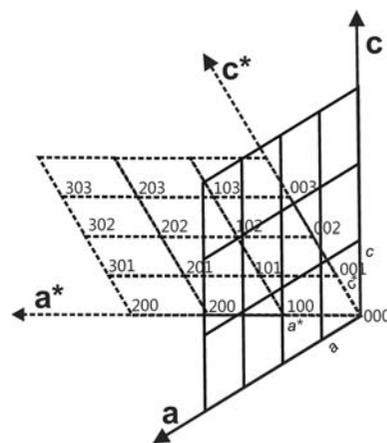

Figure 1.1.5
A two-dimensional monoclinic lattice and its corresponding reciprocal lattice. [Adapted from Dinnebier & Billinge (2008) with permission from the Royal Society of Chemistry.]

for describing all kinds of diffraction phenomena occurring in powder diffraction.

Consider a 'normal' crystal lattice with lattice vectors $\mathbf{a}$, $\mathbf{b}$ and $\mathbf{c}$, which have lengths a, b and c, respectively, and angles α between $\mathbf{b}$ and $\mathbf{c}$, β between $\mathbf{a}$ and $\mathbf{c}$ and γ between $\mathbf{a}$ and $\mathbf{b}$. The unit-cell volume is given by V. A second lattice with lattice parameters a^*, b^*, c^*, α^*, β^*, γ^* and unit-cell volume V^* with the same origin exists such that

$$\mathbf{a} \cdot \mathbf{b}^* = \mathbf{a} \cdot \mathbf{c}^* = \mathbf{b} \cdot \mathbf{c}^* = \mathbf{a}^* \cdot \mathbf{b} = \mathbf{a}^* \cdot \mathbf{c} = \mathbf{b}^* \cdot \mathbf{c} = 0,$$
$$\mathbf{a} \cdot \mathbf{a}^* = \mathbf{b} \cdot \mathbf{b}^* = \mathbf{c} \cdot \mathbf{c}^* = 1. \qquad (1.1.10)$$

This is known as the reciprocal lattice[1] (Fig. 1.1.5), which exists in so-called reciprocal space. As mentioned above, we will see that it turns out that the points in the reciprocal lattice are related to the vectors defining the crystallographic plane normals. There is one point in the reciprocal lattice for each set of crystallographic planes, (hkl), separated by distance d_{hkl}, as discussed below. For now, just consider h, k and l to be integers that index a point in the reciprocal lattice. A reciprocal-lattice vector $\mathbf{h}_{hkl}$ is the vector from the origin of reciprocal space to the reciprocal-lattice point for the plane (hkl),

$$\mathbf{h}_{hkl} = h\mathbf{a}^* + k\mathbf{b}^* + l\mathbf{c}^*, \quad h, k, l \in \mathbb{Z}. \qquad (1.1.11)$$

where $\mathbb{Z}$ is the set of all integers.

The length of the reciprocal basis vector $\mathbf{a}^*$ is defined according to

$$\mathbf{a}^* = x(\mathbf{b} \times \mathbf{c}), \qquad (1.1.12)$$

where the scale factor x can easily be deduced, using equations (1.1.12) and (1.1.10), as

$$\mathbf{a}^* \cdot \mathbf{a} = x(\mathbf{b} \times \mathbf{c} \cdot \mathbf{a}) = xV \Rightarrow x = \frac{1}{V}, \qquad (1.1.13)$$

leading to

$$\mathbf{a}^* = \frac{1}{V}(\mathbf{b} \times \mathbf{c}), \quad \mathbf{b}^* = \frac{1}{V}(\mathbf{c} \times \mathbf{a}), \quad \mathbf{c}^* = \frac{1}{V}(\mathbf{a} \times \mathbf{b}) \qquad (1.1.14)$$

and, *vice versa*,

---

[1] The reciprocal lattice is a commonly used construct in solid-state physics, but with a different normalization: $\mathbf{a} \cdot \mathbf{a}^* = 2\pi$.